An Ultra-High Power Two-Phase Jet-Impingement Avionic Clamshell Module

Murray E. Johns[†]

Issam Mudawar[††]

Electronic Cooling Research Center,
Boiling and Two-Phase Flow Laboratory,
School of Mechanical Engineering,
Purdue University, West Lafayette,
IN 47907

Boiling jet impingement heat transfer from a simulated electronic chip to Fluorinert FC-72 within a clamshell avionic module was investigated for dependence upon inlet fluid temperature, nozzle diameter, nozzle to chip spacing, jet velocity, and chip length. The clamshell module was designed and fabricated to accommodate both single and multiple chip boards and to demonstrate the feasibility of an ultra-high power (on the order of several kilowatts) module. Critical heat flux (CHF) was found to be directly dependent upon subcooling and jet velocity, but relatively unaffected by the nozzle to chip spacing variations examined. The effect of varying the chip size was evaluated and found to produce higher CHF values as chip size was decreased. A correlation accounting for both geometric and subcooling effects was adapted to predict the CHF database with a mean absolute error of 9.6 percent. The module is shown to be capable of dissipating a heat load of 12,000 W at a module flow rate of 8.01 × 10^{-4} m^3/s (12.7 gpm), thus eclipsing the current technology available in avionic cooling.

1 Introduction

It has been predicted, and current technological trends are bringing about the realization of those predictions, that high-density electronic packaging arrangements will require increasingly effective cooling schemes. Researchers have watched the almost exponentially growing ratio of power dissipation per chip to micro-electronic circuit size and have estimated that cooling requirements on the order of one hundred Watts per square centimeter and several hundred Watts per electronic array or module will necessitate improved thermal energy removal techniques by the close of the twentieth century (Mackowski, 1991). Without sufficient cooling, electronic circuit performance degradation and failure rate both increase drastically relative to the those within the designed operating temperature range.

Up until the last few years, most high-power dissipating technologies have been adequately cooled by both natural and forced convection using air as the working fluid. Other cooling packages, such as the Thermal Conduction Module (TCM) designed by IBM, have incorporated multi-mode heat transfer principles; conduction and forced liquid convection in a cold plate remove the energy dissipated by an array of micro-electronic chips (Chu, 1986). Similarly, Cray Research employed immersion cooling in the liquid-filled CRAY-2 supercomputer.

However, all of the aforementioned cooling designs operate in single phase heat transfer modes. While it is understood that natural liquid convection can greatly enhance the rate of energy dissipation over that achievable through natural air convection, the concept of boiling heat transfer merits serious consideration. As a result of the boiling process on a heated surface, the incremental increase in surface temperature with increasing heat flux to the surface is much smaller than the temperature increase associated with an identical heat flux increase in a purely single phase heat transfer situation.

Issues that complicate the requirements and characteristics of both single- and two-phase cooling arrangements include the geometric constraints placed upon the cooling system and the hardware necessary to implement the concept (e.g., fans, pumps, condensers, etc.). The synergy manifest between the thermal performance of avionics modules standard to several military platforms and the restricted geometry of such modules has pushed researchers to develop module concepts that incorporate improved energy removal rates in anticipation of increasing high power-dissipating conditions. Concept proposals for new avionics modules have included cooling arrangements that feature conduction and air or liquid cooling in indirect contact with the chips. Figure 1 reveals the cross sections of these elementary arrangements.

Edge-air cooling, Fig. 1(*a*), requires that dissipated power be conducted from the chips through the module and into a cold plate cooled by air bled from the engine compressor. The thermal resistances associated with such an arrangement impose a relatively low upper-threshold upon the configuration's potential to dissipate power. The second cooling concept, shown in Fig. 1(*b*) improves upon the first by incorporating an air flow path through the module frame as a more effective means of thermal energy removal; it too, however, employs indirect cooling and is deemed insufficient for anticipated thermal requirements. Figures 1(*c*) and 1(*d*) show cooling schemes identical to those in Figs. 1(*a*) and 1(*b*) with the exception that the cold plate and flow-through module are liquid cooled. Not one of these configurations actually features direct immersion of the chips in the working fluid. Consequently, edge air-cooled modules have been demonstrated to dissipate a mere 40 Watts per module while a liquid flow through module has been shown to dissipate about 200 Watts (Barwick et al., 1991). However, direct immersion and forced convection cooling can greatly enhance a module's capability to dissipate even larger heat fluxes by eliminating portions of the thermal resistance bridge associated with indirect cooling methods. A module incorporating direct immersion cooling with a liquid working fluid is shown in Fig. 1(*e*). The liquid not only cools the cold plates but also circulates through the module in direct contact with the electronic circuitry.

A combination of both liquid immersion and boiling heat transfer in an avionics module was proposed by Mudawar et

---

[†] Graduate student; present address: WL/FIVE Bldg. 45, 2130 Eighth St. Suite 1, WPAFB, OH 45433-7542

[††] Professor and Director of the Purdue University Boiling and Two-Phase Flow Laboratory; author to whom all correspondence should be addressed.

Contributed by the Electrical and Electronic Packaging Division for publication in the JOURNAL OF ELECTRONIC PACKAGING. Manuscript received by the EEPD March 1, 1994; revised manuscript received February 13, 1995. Associate Technical Editor: B. G. Sammakia.

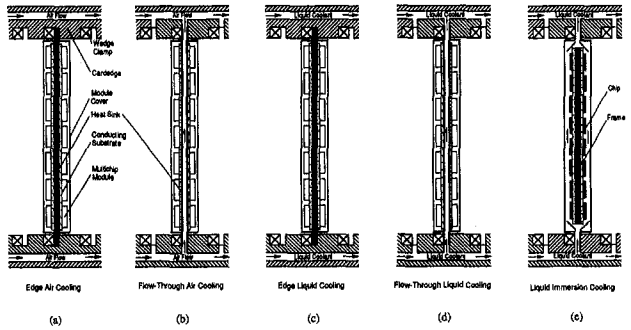

Fig. 1 Avionic cooling schemes featuring (a) conduction cooled center frame (heat sink) module clamped to air cooled cardcage rail, (b) air flow-through center frame module, (c) conduction cooled center frame module clamped to liquid cooled cardcage rail, (d) liquid flow-through center frame module and (e) liquid immersion chip-on-board module.

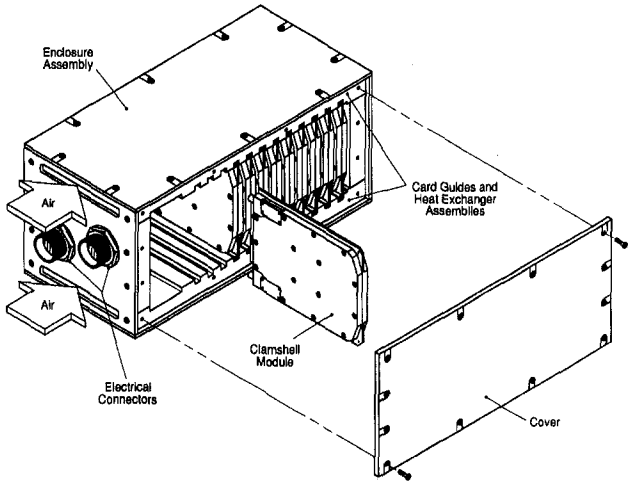

Fig. 2 Mounting of clamshell modules in an avionics enclosure

al. (1994). The module was designed for the U.S. Navy to satisfy the geometrical packaging requirements of the Standard Electronic Module—type E (SEM-E) and to dissipate at least 500 W. The first module design, the BTPFL-C1 (Boiling and Two-Phase Flow Laboratory—Clamshell Module 1), was primarily an open cavity through which the dielectric coolant, Fluorinert FC-72 produced by 3M, would circulate at very low speed over the surfaces of several chips populating a circuit board. This particular module was shown to be capable of dissipating more than 800 W while maintaining chip temperatures below 80°C. In order to examine the potential of a similar module with a more aggressive cooling scheme, the BTPFL-C2 was developed to incorporate relatively high velocity coolant flow in small channels formed directly at the chip surfaces (Jimenez and Mudawar, 1994). As a result of this module enhancement, the BTPFL-C2 was shown to be capable of dissipating in excess of 3000 W using approximately 3.2×10^{-5} m^3/s (0.5 gpm) of coolant at an inlet subcooling of 40.3°C and suffering a pressure drop of only 2800 N/m^2 (0.41 psi). These modules, referred to as "clamshell" modules as a consequence of the module design, were projected to meet the physical constraints of standard avionic enclosures such as that shown in Fig. 2.

In order to improve upon the cooling advancements made through the design of both the BTPFL-C1 and BTPFL-C2 modules, a third generation module is proposed in the present study. The proposed design of the BTPFL-C3 module would employ larger coolant flow rates that would be routed within the module in such a manner as to impinge as confined circular liquid jets upon the surfaces of the chips. The cooling performances of the BTPFL-C1 and BTPFL-C2 modules are limited significantly by the small outer envelope of the sleeveless couplers used to deliver fluid to and from the module; both modules were single pitch SEM-Es with a thickness of only 1.5 cm. The couplers contain several internal seals designed to prevent coolant spillage or air inclusion during insertion of the module into the avionic enclosure, as well as intricate mating surfaces to preclude misalignment between the coupler's mating parts. The delicate design of the couplers and their small outer envelope, up to 1.5 cm, place an upper limit on coolant flow rate of about 3.2×10^{-5} m^3/s (0.5 gpm) for single pitch modules. It is possible to greatly relax this constraint by utilizing a dual pitch module which would still conform to the packaging constraints of standard avionic enclosures. A dual pitch module would provide room for both larger couplers and thicker walls. Since pressure drop is proportional to flow passage diameter to the negative 4th power, doubling the outer envelope of the couplers should allow a 16 fold increase in the coolant flow rate for the same pressure drop. With the additional wall strength and corresponding increase in allowable pressure drop with a dual pitch module, it is possible to increase the flow capacity of the module to about 9.5×10^{-4} m^3/s (15 gpm).

The objectives of this study are as follows:

(1) Develop a double pitch avionics module capable of employing boiling jet impingement cooling and sized to follow the SEM-E guidelines and to house a multitude of simulated electronic chips.
(2) Demonstrate that this avionics module is capable of dissipating heat in the range of several kilowatts.

Nomenclature

c_p = specific heat at constant pressure
CHF = critical heat flux, q''_m
d = nozzle diameter
h_{fg} = latent heat of vaporization
H = nozzle to chip spacing
L_h = length of square chip (4.23, 6.35, or 12.7 mm)
P = pressure
ΔP = pressure drop across jet (or module)
q'' = average chip heat flux
q''_m = critical heat flux
q''_* = dimensionless CHF
$q_{m,chip}$ = heat dissipation per chip at CHF
$q_{m,mod}$ = heat dissipation per module at CHF
$\Delta T_{sub,i}$ = inlet liquid subcooling, $T_{sat} - T_i$
ΔT_w = temperature difference between the chip surface and inlet liquid, $T_w - T_i$
U_n = mean liquid nozzle velocity
$\dot{V}_{chip}$ = coolant flow rate per chip
$\dot{V}_{mod}$ = coolant flow rate for entire module
We = Weber number, $[\rho_f U^2 (L_h - d)]/\sigma$

Greek Symbols

ρ = density
σ = surface tension

Subscripts

f = liquid
g = vapor
i = inlet to upstream nozzle plenum
sat = saturated condition
sub = subcooled condition
w = mean chip surface condition.

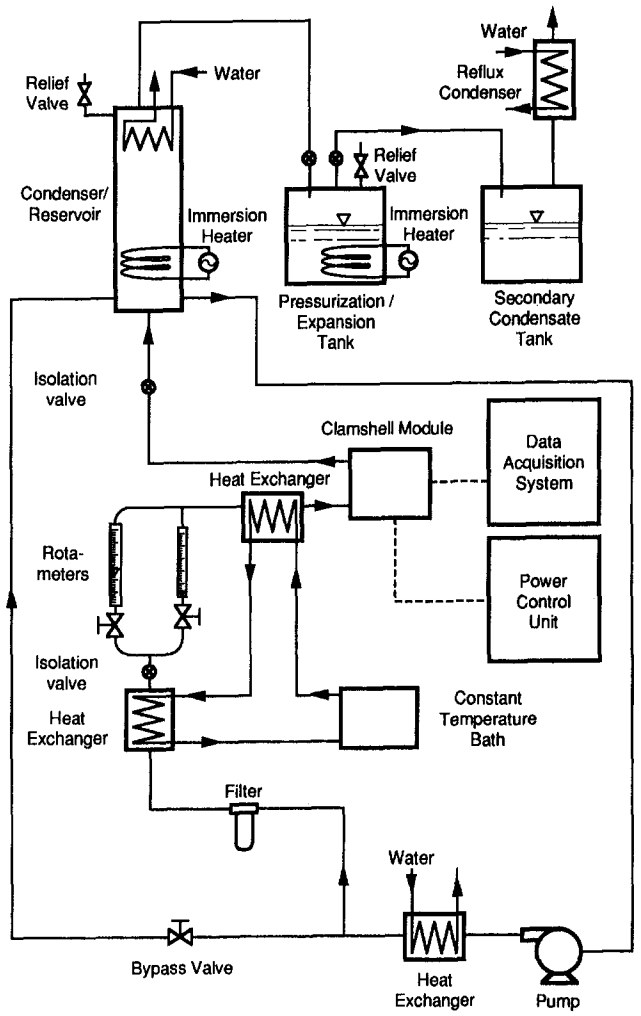

Fig. 3 Two-phase flow loop

(3) Ascertain the parametric trends of submerged liquid jet cooling by examining the effects of varying nozzle diameter, jet velocity, chip length and liquid subcooling, and develop a correlation for critical heat flux that would enable a design engineer to determine upper cooling limits for the module.

2 Experimental Methods

Flow Loop. The dielectric working fluid in this study, FC-72, was conditioned to the desired module inlet temperature and module outlet pressure by a closed two-phase flow loop. As shown in Fig. 3, the fluid was circulated in the loop by a magnetically coupled, centrifugal pump. In order to maintain flow stability and to avoid very high pressures within the module, only a fraction of the total flow entered the module while the rest was routed through a bypass line. In addition, the volumetric flow rate in the module, and hence the fluid velocity through the jet, was controlled by a regulating needle valve located just upstream of the module inlet. The flow rate of the fluid passing through the module was measured by one of two rotameters depending on the magnitude of the flow rate in a particular experiment.

Inlet fluid temperature was maintained by three heat exchangers. The first heat exchanger, located immediately downstream of the pump, was used to remove excess thermal energy supplied to the flow by the module, pipe friction and pump work. The second and third heat exchangers were located on either side of the rotameters to fine tune the fluid temperature prior to entering the module. The effect of the latter two heat exchangers was regulated with a constant temperature bath. Upon exiting the module, the fluid entered the condenser/reservoir where it recombined with the fluid from the bypass line and subsequently returned to the pump. Water flow through the condenser was regulated by a solenoid valve which maintained the module outlet pressure at the desired value. In addition, a filter in the bypass line removed impurities from the fluid that could block the jets in the module or otherwise degrade the flow loop's performance.

Chip Design. The simulated chips, machined from oxygen-free copper, were designed to expose surface areas of 12.7×12.7 mm^2 (0.50×0.50 in^2), 6.35×6.35 mm^2 (0.25×0.25 in^2) and 4.23×4.23 mm^2 (0.167×0.167 in^2) to the fluid flow for the full-, medium- and small-size chips, respectively. A thick-film resistor of approximately 90 Ω was soldered to the underside of each copper chip. Four Chromel-Alumel thermocouples were inserted below the boiling surface of the full-size chip at a depth of 3.06 mm (0.12 in.) and were positioned to provide an adequate representation of the surface temperature profile. Similarly, two Chromel-Alumel thermocouples were located at the center and at a corner (0.5 mm into the wetted square) beneath the surface of the medium-size chip as well as below that of the small-size chip. For all three chip sizes, a one-dimensional heat conduction analysis was used to calculate the surface temperature above each of the thermocouples, and an area-weighted average of the corrected surface temperatures established the mean surface temperature. The holes for the thermocouples were drilled into the chip at locations which evenly distributed the removed mass around the body of the chip.

Design and Fabrication of the BTPFL-C3 Module. The flow and space requirements for jet impingement cooling suggested the BTPFL-C3 module thickness be twice that of the previous modules. This permitted the BTPFL-C3 design to remain compatible with standard avionic enclosures already in use in military platforms. Existing enclosures (see Fig. 2) would merely require the appropriate mating fluid and electrical couplers for the dual-thickness module. Both aluminum 7075-T6 and 6061-T6 alloys are incorporated into the design of the different components of the BTPFL-C3 module.

The characteristics of jet impingement cooling, strongly dependent upon the impinging coolant's temperature, are maintained by keeping the fresh and spent coolant from mixing. Consequently, the BTPFL-C3 module design incorporates several sealing surfaces that allow fresh coolant to enter the module and pass through the jet impingement zone to the outlet as warmed and vaporized fluid without directly contacting any of the upstream flow.

The primary component of the module has the appearance of a frame; as manifest in Fig. 4, the sides and faces are shaped to accommodate the other layered components, electrical and fluid couplers and o-ring seals, while the center remains open through the complete thickness of the frame. The other "layers" can be best explained by proceeding from the inside of the module to the outside (symmetry allows the discussion of a single side of the module). A high-temperature fiberglass-epoxy circuit board is inserted through a slot in the center of the frame just as a portrait would be inserted into a picture frame; the electronic chips on each side of the circuit board (in a multi-chip situation) face a jet impingement plate which is channeled and shaped on each side to allow both inlet and outlet flow to pass. The jet plate is pressed against an o-ring seal by a cover plate which also seals against an o-ring in its own plane. The cover plates, one on each side of the module, are fastened to each other with socket-head cap screws that pass through the module frame to compress and hold the rest of the layers in place.

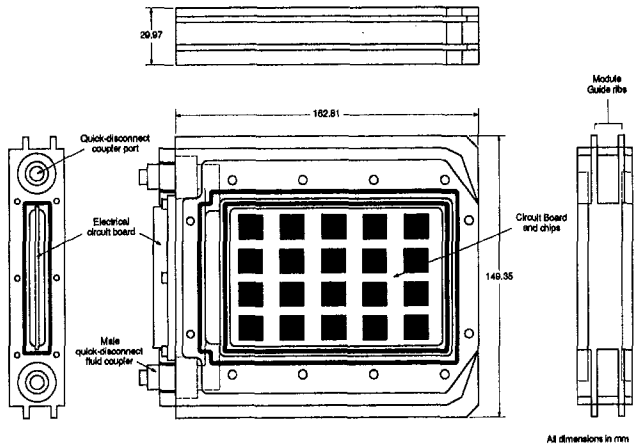

Fig. 4 BTPFL-C3 module (without cover plates)

Whereas a circuit board populated with chips on both sides would allow symmetry to simplify the analysis, a single-chip parametric study of several geometric cooling configurations required that fluid flow be restricted to only one side of the module; the opposite side of the circuit board faced a dummy orifice plate as shown in Fig. 5. This restriction upon the flow path ensured a consistent knowledge of the liquid mass flow rate arriving at the chip surface.

In order to determine the optimum geometric configuration for the jet-impingement cooling scheme implemented in the BTPFL-C3 module, several jet plates were fabricated to permit the variation of both jet diameter and nozzle to chip spacing. Jet plates were fabricated for jet diameters of 0.40 mm (0.0156 in.), 0.79 mm (0.0312 in.) and 2.06 mm (0.081 in.). To maintain consistent flow conditions for the different diameters, the jet plates were designed to provide the same flow development length for each jet diameter.

Operating Procedure. In order to maintain surface uniformity between experiments, the chip surface exposed to the fluid flow was blasted with a water-particulate slurry preceding a set of experiments. Jet impingement was found to be sufficiently erosive as to adequately clean the chip surfaces of most potential deposits, thus precluding the need to vapor blast the surfaces prior to each experiment. The slurry particles had an average size of 10 μm and served to create a uniform surface texture on each chip.

The system was deaerated before experiments were conducted in order to remove noncondensible gases from the FC-72 fluid and, thus, to ensure consistent fluid properties from experiment to experiment. Deaeration was accomplished by heating the fluid to saturation with the system open to the atmosphere. As the fluid was heated, FC-72 vapor and noncondensible gases were routed from the flow loop to a water-cooled reflux condenser. The condenser allowed the noncondensible gases to escape to the ambient while the FC-72 condensed and dripped back into a condensate tank.

For the three different nozzle diameters tested, 0.40 mm (0.0156 in.), 0.79 mm (0.0312 in.) and 2.06 mm (0.081 in.), data were taken at jet velocities of 0.5, 1.0, 2.0, 3.0, 4.0, 5.0 and 6.0 m/s. The effects of subcooling were examined at 10, 25 and 40°C. At each velocity, the power dissipated by the chip was slowly incremented through the complete boiling curve until CHF was attained.

The data acquisition system looped through a routine that updated all measurements approximately every three seconds. However, one thermocouple temperature was monitored much more frequently to anticipate critical heat flux. Power control modules were controlled by the system to shut off the chip power when the chip temperature exceeded a preset maximum.

The saturation pressure for the simulated chip was taken to be the pressure in the fluid outlet plenum. This outlet pressure was maintained at near 1.24×10^5 N/m^2 (18.0 psia) in all experiments to ensure a common reference for saturation properties at the outlet. Inlet subcooling was then calculated as the difference between the saturation temperature (62.8°C) corresponding to the outlet pressure and the fluid temperature just upstream of the jet.

Each data point was taken after the system attained a steady-state condition. Generally, steady-state was recognized when all of the thermocouple temperatures and the upstream fluid inlet temperature had several consecutive readings with fluctuations of no more than ±0.1°C. Near CHF, the heat flux increments were decreased to at most 1.0 W/cm^2 to ensure that CHF was not reached prematurely. Critical heat flux was approximated as the last stable heat flux above which a small increment in the power instigated a rapid temperature increase. Critical heat flux could thus be isolated within 1.0 W/cm^2.

Experimental Uncertainty. The maximum uncertainty associated with the thermocouple measurements was estimated to be ±0.2°C. Similarly, the experimental uncertainties reported by the manufacturer of the pressure transducers was ±1030 N/m^2 (±0.15 psi). Heat sources mounted in a similar fashion to that of the present study have been analyzed for heat losses to the mounting substrate; the heat losses have proven to be on the order of 1 percent of the total heat dissipation (Mudawar, et al., 1994). Likewise, uncertainty associated with the power measurement is estimated at less than 5 percent and that of the flow meter readings at 1.6 percent.

3 Results

Subcooling Effects and Their Impact on Thermal Management in Avionics. Subcooled liquid aids the condensation and collapse of bubbles formed during the boiling process. Complete condensation of the vapor prior to exiting the module facilitates both pumping and conditioning considerations; a fluid conditioning loop for avionic cooling is typically constructed to handle the liquid phase only. Such single phase pumping situations are highly desirable to limit the equipment components required for proper fluid conditioning. Similarly, rapid condensation of the vapor produced during boiling can decrease the sensitivity of boiling systems subject to fluctuating body forces such as those experienced in aircraft flight.

In addition, as the inlet subcooling is increased, the onset of nucleate boiling is delayed to higher heat fluxes and heater surface temperatures. This phenomenon is a result of the increased sensible heat available, through the increased subcooling, to transport energy from the chip surface before saturation conditions are reached within the flow. Figure 6 displays boiling curves for three cases conducted under identical conditions save for the subcooling. The trend toward an increased delay in the

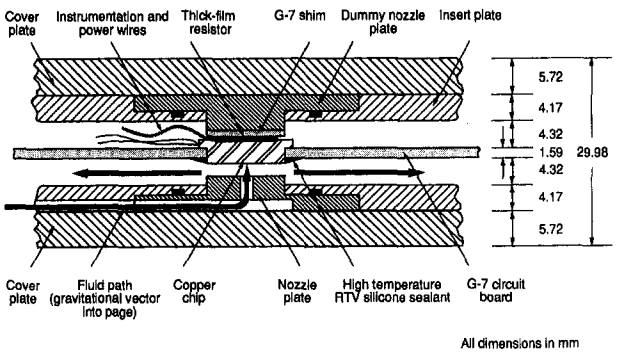

Fig. 5 Cross section of single chip arrangement inside BTPFL-C3 module

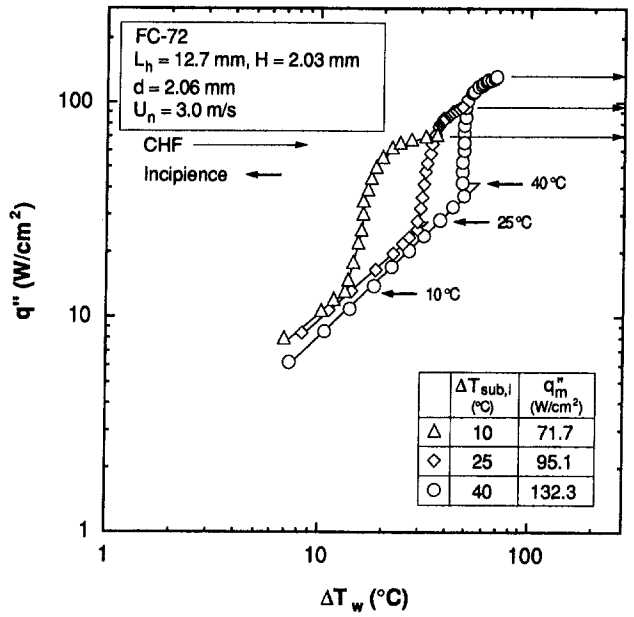

Fig. 6 Delay of onset of nucleate boiling and increase of CHF with increased subcooling

onset of nucleate boiling, which onset is marked by a large increase in the slope of a boiling curve, is clearly evident in Fig. 6. Maddox and Mudawar (1989) observed this phenomenon and reported that increased subcooling reduced both the vapor bubble departure diameter and the thickness of the bubble layer covering a chip surface. They concluded, consequently, that as subcooling increased, there was greater opportunity for liquid to penetrate the vapor layer and make contact with the chip surface. As a result, CHF was delayed to higher heat fluxes.

Similarly, a rapid drop in the chip's temperature associated with the incipience of nucleate boiling is also seen to depend on subcooling. This incipience temperature drop is the consequence of sudden boiling activation of inactive nucleation sites that occurs as the vapor from the first activated sites spreads and invades nearby cavities to provide the initial vapor embryos necessary for bubble growth. Incipience temperature drop, therefore, is decreased by increased subcooling as a result of the suppression of vapor bubble growth. Near-saturated conditions, however, will allow the vapor bubbles to grow and invade neighboring sites. Consequently, the rapid activation of boiling sites very quickly decreases the heated surface temperature. However, this sudden temperature fluctuation is undesirable in the performance of boiling systems designed to cool electronic circuits; thermal cycling, especially the large temperature excursions possible as a result of this incipience-associated phenomenon, is extremely detrimental to the performance and life of typical electronic chips. While not immediately evident in the data presented in Fig. 6, the trend of decreasing incipience temperature drop with increasing subcooling was widely present in the general data base.

Effect of Nozzle to Heater Spacing. In an attempt to evaluate the dependence of boiling jet impingement heat transfer on the spacing between the nozzle outlet and the heater surface, three tests were conducted under conditions identical in all variables except the nozzle to chip spacing, H. While Nonn et al. (1988) witnessed increased critical heat flux magnitudes as H was decreased below 0.5 mm (0.02 in.), they did report that no change in CHF was observed for H values between 0.5 mm (0.02 in.) and 5 mm (0.2 in.). Mudawar and Wadsworth (1991) investigated nozzle to chip spacing for confined rectangular jets over the range $0.508 \leq H \leq 5.08$ mm ($0.02 \leq H \leq 0.20$ in.) and found the effect upon CHF to be weak in the medium velocity range ($1.5 \leq U_n \leq 7$ m/s) but pronounced at higher velocities. The values of H (0.51, 1.02 and 2.03 mm) and U_n (3.0 m/s) chosen for the three varied-spacing experiments of the present study fell within the ranges evaluated by Mudawar and Wadsworth. Similar to their findings, little difference in the CHF values was witnessed for the three values of H that were evaluated.

Effect of Chip Size. Three different chip sizes were examined under identical conditions in order to determine the effect that changing the chip size may have on the boiling characteristics and critical heat flux of an impinging jet. Figure 7 reveals the differences seen between the boiling curves produced by each of the three chips. It is evident from the results displayed in Fig. 7 that, as the chip length was decreased, the CHF correspondingly increased.

Estes and Mudawar (1994) found that dryout on a heated surface subject to an impinging, free-surface liquid jet occurred first at the edges of the heater and then gradually approached and enveloped the central region of the heater as power to the heater was slowly increased. This behavior is the result of increased void fraction within the wall jet; the increase precludes a coherent liquid continuum in the wall jet liquid. Consequently, much of the wall jet is broken up and vigorously pushed away from the heated surface by splashing effects. Therefore, for a fixed flow rate and a particular nozzle diameter, as chip length decreases, the chip boundaries furthest from the point of stagnation are placed into regions of decreasing void fraction and, consequently, lessening danger of dryout relative to the boundaries of larger chips. As a result, CHF is delayed to higher heat fluxes as chip length is decreased. While jet confinement in the present study aids in resisting wall jet breakup, the detrimental effect of increasing the chip length is clearly evident.

Effect of Mean Jet Velocity. Mean jet velocity, termed to signify the average of the velocity profile in the nozzle, was simply calculated from a knowledge of the nozzle diameter and the liquid volumetric flow rate through the nozzle. For each nozzle diameter, several mean jet velocities were examined at each subcooling. Figure 8, for example, demonstrates the boiling curves for all seven velocities (0.5, 1, 2, 3, 4, 5 and 6 m/s) evaluated for a nozzle diameter of 2.06 mm (0.081 in.) at 25°C subcooling. While the seven curves merge in the nucleate boiling regime, the single phase regime reveals the different

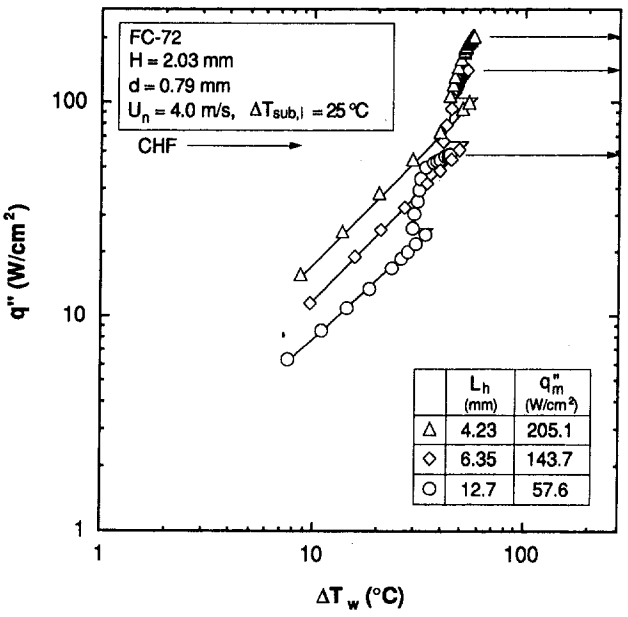

Fig. 7 Effect of chip length on CHF

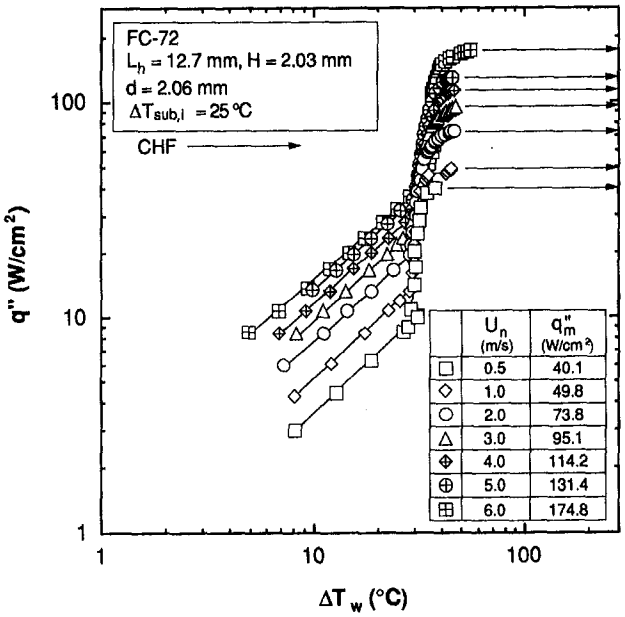

Fig. 8 Boiling curves for different jet velocities

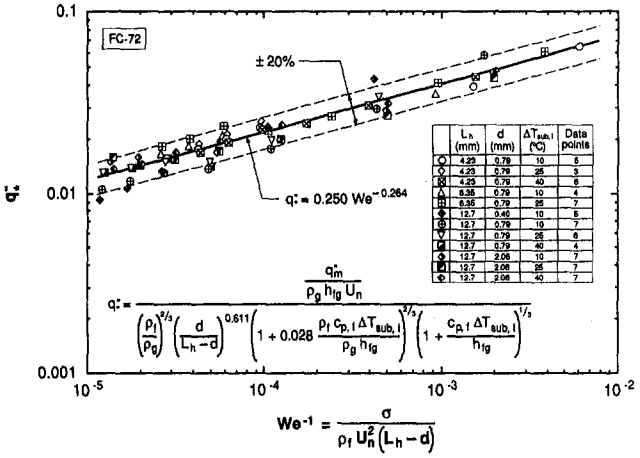

Fig. 9 Correlation of CHF data

heat transfer coefficients associated with each of the respective velocities. Figure 8 also makes obvious the fact that increasing jet velocity generally increases the critical heat flux attainable under identical subcooling conditions.

CHF Correlation. In order to provide a design tool for future use in jet impingement applications, the CHF data for the single chip experiments, a total of 68 experimentally-determined values, were correlated by an expression involving dimensionless groups accounting for the ratio of surface tension to inertial forces (inverse Weber number), geometric parameters including the chip length and nozzle diameter, the liquid to vapor density ratio, and the effect of subcooling. The correlation, having a general form adapted from that reported by Mudawar and Wadsworth (1991) for confined, rectangular jets is expressed as (see Johns, 1994)

$$q''_* = \frac{\dfrac{q''_m}{\rho_g h_{fg} U_n}}{\left(\dfrac{\rho_f}{\rho_g}\right)^{2/3}\left(\dfrac{d}{L_h - d}\right)^{0.611}\left(1 + 0.028\,\dfrac{\rho_f c_{p,f}\Delta T_{sub,i}}{\rho_g h_{fg}}\right)^{2/3}\left(1 + \dfrac{c_{p,f}\Delta T_{sub,i}}{h_{fg}}\right)^{1/3}} = 0.250\left(\frac{\sigma}{\rho_f U_n^2 (L_h - d)}\right)^{0.264} \quad (1)$$

The correlation fits the experimental data with a mean absolute deviation of 9.6 percent, as shown in Fig. 9. Because the present data were determined for a fairly constant density ratio ($101.2 \le \rho_f/\rho_g \le 104.8$), the exponent of the density ratio term, as previously recommended by Mudawar and Wadsworth, was fixed at $\frac{2}{3}$.

4 Cooling Performance of BTPFL-C3

Implementation of the BTPFL-C3 in avionic cooling places upper limits on several key parameters that could influence CHF in the jets. These limits include restricting jet velocity below 10 m/s to avoid erosion on the chip surface and controlling the flow in the module to maintain the pressure drop below about 2.1×10^5 N/m^2 (30 psi), a condition easily sustained in most experiments conducted in the present study. Furthermore, the fluid couplers sized for the dual pitch BTPFL-C3 place an upper limit on coolant flow rate of about 9.5×10^{-4} m^3/s (15 gpm).

For example, the module's total heat load capability can be assessed from calculations based upon a proposed population of forty, 12.7 × 12.7 mm^2 chips (twenty on each side of the circuit board). Given the maximum critical heat flux attained in the present study for the largest chip (185 W/cm^2 for d = 2.06 mm, $\Delta T_{sub,i}$ = 40°C and U_n = 6 m/s), the module could potentially dissipate 12,000 W at a flow rate requirement of 8.01×10^{-4} m^3/s (12.7 gpm). Obviously, a more systematic method is desired to aid the design engineer in deciding which operating conditions are best suited for a given avionics system. Outlined below is a generalized method for these design purposes.

Figures 10(*a-c*) show, for an operating pressure of 1.52×10^5 N/m^2 (22 psi), recommended by Mudawar et al. (1994) for avionic clamshell modules, and three values of inlet subcooling, performance plots based on Eq. (1) for the BTPFL-C3 module populated with the same forty chips. They include the module's peak cooling rate, q_{mod}, and pressure drop (assuming total loss of the velocity head of the impinging fluid), ΔP, for different jet diameters and flow rates. Each of these figures illustrates a very attractive attribute of jet impingement: higher module heat dissipation is possible for the same flow rate simply by decreasing nozzle diameter due to a greater sensitivity of critical heat flux to jet velocity than to flow rate. While this feature points to the advantage of greatly reducing jet diameter, Figs. 10(*a-c*) also point to a drastic increase in pressure drop with decreasing jet diameter. Comparing the three figures reveals decreasing the inlet temperature (i.e., increasing the subcooling) broadens the module's peak cooling rate envelope significantly.

Figure 11 compares the peak cooling rates for the various military SEM-E modules developed to date. The cooling performance of the modules utilizing subcooled boiling is clearly shown to be drastically better than that of the indirect liquid-cooled frame recently developed by the Air Force (Barwick et al., 1991). Similarly, all four liquid-cooled modules are superior in cooling performance relative to modules cooled by conduction alone. Of the five types of modules, the BTPFL-C3, with its high flow rate and use of jet impingement boiling, is the only module capable of extending the peak cooling potential of

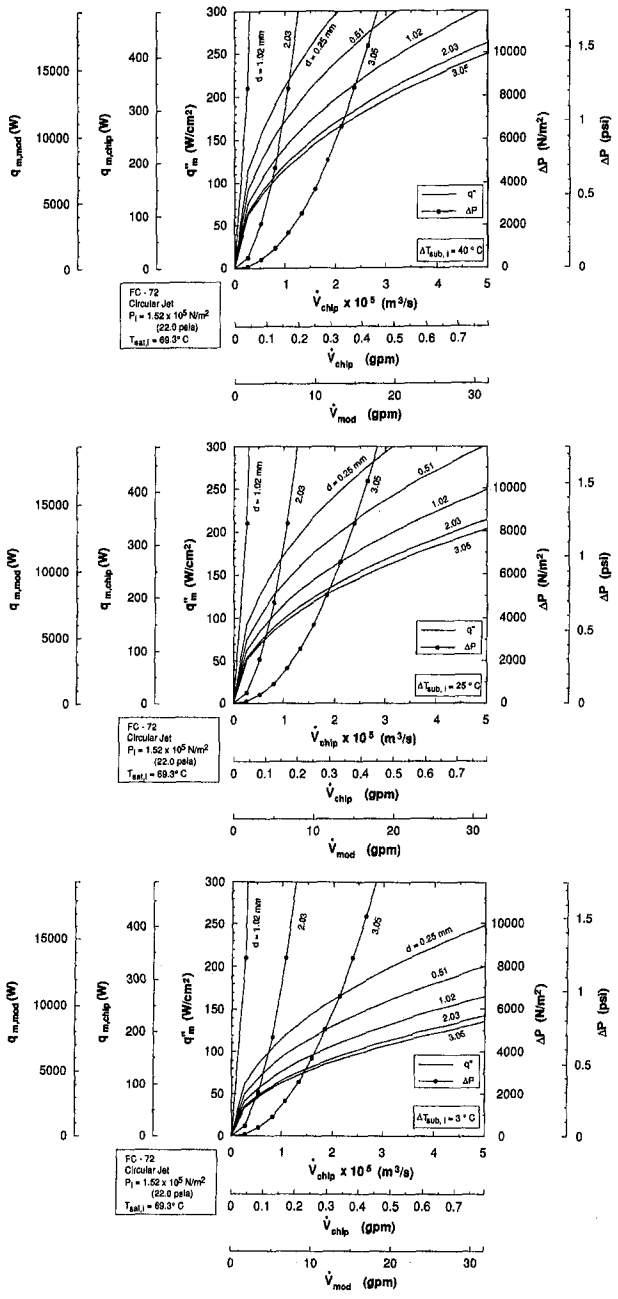

Fig. 10 Projection of BTPFL-C3 performance for inlet subcooling of Fig. 10(*a*) 40, Fig. 10(*b*) 25, and Fig. 10 (*c*) 3°C for a module housing a double-sided circuit board with each side carrying 20 of 12.7 × 12.7 mm^2 chips

SEM-Es above 10 kW, over three hundred times that of today's conventional conduction cooled modules.

5 Summary

The present study explored the implementation of confined jet impingement in cooling ultra-high power avionics. Primary conclusions from this investigation are as follows:

(1) Employing a highly subcooled flow in avionic modules is crucial for aiding in the condensation and collapse of bubbles formed on the chip surfaces, thus both greatly simplifying the coolant conditioning outside of the module and decreasing the sensitivity to fluctuations in body force encountered in military aircraft. Increasing subcooling and jet velocity serve to increase both the single-phase heat transfer coefficient and CHF and reduce hysteresis effects.

(2) No significant change in CHF was experienced for the nozzle-to-heater spacings examined.

(3) CHF increased with decreasing chip length as a consequence of the relative decrease in void fraction encountered by the wall jet on smaller chips.

(4) A new CHF design correlation was constructed which predicted the experimental data with a mean absolute error of 9.6 percent.

(5) The BTPFL-C3 eclipsed all existing SEM-E modules by extending the peak cooling potential above 10 kW, over three hundred times the cooling rate of today's conventional conduction cooled modules.

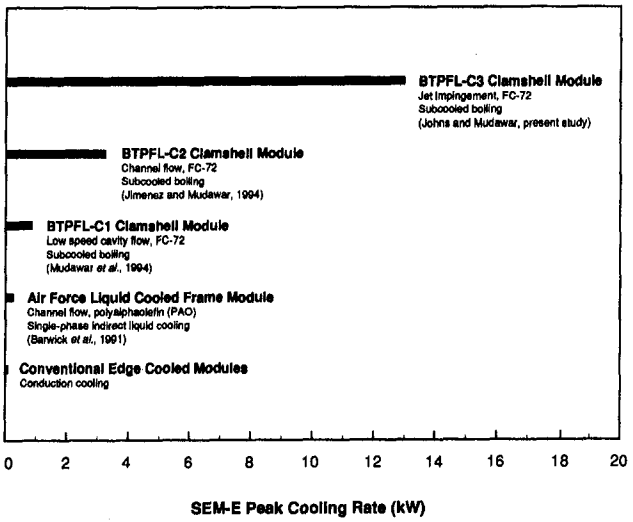

Fig. 11 Comparison of peak cooling rates for military SEM-E modules

References

Barwick, M., Midkiff, M., and Seals, D., 1991, "Liquid Flow-Through Cooling For Avionics Applications," *IEEE National Aerospace and Electronics Conf.*, Vol. 1, Dayton, OH, pp. 227–230.

Chu, R. C., 1986, "Heat Transfer in Electronic Systems," *8h Int. Heat Transfer Conf.*, C. L. Tien, V. P. Carey, and J. K. Ferrell, ed. Vol. 1, San Francisco, CA, pp. 293–305.

Estes, K., and Mudawar, I., 1995, "Comparison of Two-Phase Electronic Cooling Using Free Jets and Sprays," ASME JOURNAL OF ELECTRONIC PACKAGING, Vol. 118, pp. 127–134.

Jimenez, P. E., and Mudawar, I., 1994, "A Multi-Kilowatt Immersion-Cooled Standard Electronic Clamshell Module for Future Aircraft Avionics," ASME JOURNAL OF ELECTRONIC PACKAGING, Vol. 116, pp. 220–229.

Johns, M. E., 1994, "Application of Jet Impingement Boiling in an Ultra-High Power Avionic Clamshell Module," Masters thesis, School of Mechanical Engineering, Purdue University, West Lafayette, IN.

Mackowski, M. J., 1991, "Requirements for High Flux Cooling of Future Avionics Systems," *Aerospace Technology Conf. and Exposition,* Long Beach, CA, SAE Paper No. 912104.

Maddox, D. E., and Mudawar, I. A., 1989, "Single and Two-Phase Convective Heat Transfer from Smooth and Enhanced Microelectronic Heat Sources in a Rectangular Channel," ASME JOURNAL OF HEAT TRANSFER, Vol. 111, pp. 1045–1052.

Mudawar, I., Jimenez, P. E., and Morgan, R. E., 1994, "Immersion-Cooled Standard Electronic Clamshell Module: A Building Block for Future High-Flux Avionics Systems," ASME JOURNAL OF ELECTRONIC PACKAGING, Vol. 116, pp. 116–125.

Mudawar, I., and Wadsworth, D. C., 1991, "Critical Heat Flux from a Simulated Chip to a Confined Rectangular Impinging Jet of Dielectric Liquid," *Int. J. Heat Mass Transfer,* Vol. 34, pp. 1465–1479.

Nonn, T., Dagan, Z., and Jiji, L. M., 1988, "Boiling Jet Impingement Cooling of Simulated Microelectronic Heat Sources," ASME Paper No. 88-WA/EEP-3.